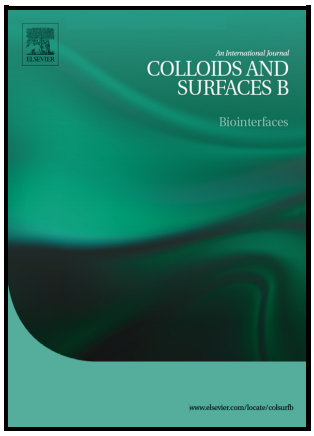

Liposomal encapsulation of crocin-rich tomato extract (Tomafran)and its in-depth evaluation as a cosmeceutical ingredient.

Maria Mondéjar-López, María Paz García-Simarro, Julia Vega, Cristian Martínez Fajardo, Susana López-López, Oussama Ahrazem, Lourdes Gómez-Gómez, Felix L. Figueroa, Enrique Niza

PII: S0927-7765(25)00273-5

DOI: https://doi.org/10.1016/j.colsurfb.2025.114766

Reference: COLSUB114766

To appear in: *Colloids and Surfaces B: Biointerfaces*

Received date: 10 March 2025
Revised date: 30 April 2025
Accepted date: 3 May 2025

Please cite this article as: Maria Mondéjar-López, María Paz García-Simarro, Julia Vega, Cristian Martínez Fajardo, Susana López-López, Oussama Ahrazem, Lourdes Gómez-Gómez, Felix L. Figueroa and Enrique Niza, Liposomal encapsulation of crocin-rich tomato extract (Tomafran)and its in-depth evaluation as a cosmeceutical ingredient., *Colloids and Surfaces B: Biointerfaces,* (2025) doi:https://doi.org/10.1016/j.colsurfb.2025.114766

Liposomal encapsulation of crocin-rich tomato extract (Tomafran) and its in-depth evaluation as a cosmeceutical ingredient.

Maria Mondéjar-López [1], María Paz García-Simarro[1], Julia Vega[2], Cristian Martínez Fajardo[1], Susana López-López[3] Oussama Ahrazem[1,4] Lourdes Gómez-Gómez[1,5], Figueroa, Felix L.[2*] and Enrique Niza[1,5,*]

[1] *Instituto Botánico. Departamento de Ciencia y Tecnología Agroforestal y Genética. Universidad de Castilla-La Mancha, Campus Universitario s/n, 02071 Albacete, Spain.*

[2] *Malaga University, Andalusian Institute of Blue biotechnology and Development (IBYDA). Experimental Center Grice Hutchinson. Lomas de San Julián, 2. 29004 Malaga, Spain*

[3]*Facultad de Medicina, Departamento de Química Inorgánica, Orgánica y Bioquímica, Universidad de Castilla-La Mancha, C/Almansa 14, 02008 Albacete, Spain*

[4]*Escuela Técnica Superior de Ingeniería Agronómica y de Montes y Biotecnología. Departamento de Ciencia y Tecnología Agroforestal y Genética. Universidad de Castilla-La Mancha, Campus Universitario s/n, 02071 Albacete, Spain.*

[5]*Facultad de Farmacia, Departamento de Ciencia y Tecnología Agroforestal y Genética.*

Abstract.

This study evaluates the potential of a genetically modified, crocin-rich tomato extract (Tomafran) as a biological photoprotector and for skin health applications. Biochemical characterization and antioxidant capacity of Tomafran were assessed. Tomafran showed lower values than saffron in the ABTS assay, but similar values in the DPPH and BCBA assays. Additionally, Tomafran reduced advanced glycation end products (AGEs) and reactive oxygen species (ROS) in human fibroblasts, which are related to the negative effects of UV radiation on the skin. The extract was encapsulated in liposomes, yielding particles with an average size of 60.96 nm, a polydispersity index (PDI) of 0.06, a zeta potential of -21.50 mV, and a spherical morphology. The liposomal formulation demonstrated storage stability and a

controlled release profile, with approximately 60% of the extract released within the first 10 hours. The photoprotective capacity, measured through sun protection factor (SPF) and other biological protection factors, showed very slight improvements with increasing concentrations of Tomafran, achieving values lower than 2. The extract showed instability against UV radiation and high temperature, although encapsulation in liposomes provided protection. The anti-inflammatory properties of the liposomal Tomafran extract were evaluated using RAW 264.7 macrophage cells, showing significant reductions in proinflammatory interleukins IL-6 and IL-12. These findings highlight Tomafran's potential for mitigating inflammation associated with oxidative stress and UV-induced skin damage.

Keywords:
Cosmeutical, crocin , liposome

1. Introduction

Ultraviolet radiation is among the most damaging external factor for the skin, which can cause various harmful effects on human health, such as the generation of reactive oxygen species (ROS), erythema, hyperpigmentation, burning, pruritus, cancer and premature skin aging [1] [2]. This ultraviolet radiation consists of the so-called UV-C (λ = 100-280 nm), UV-B (λ = 280-320 nm) and UV-A (λ = 320-400 nm) [1]. UV-B is partially absorbed by the atmosphere and only comprise 10% of the total UV radiation that reach the Earth´s surface. It can be absorbed by the epidermal cells like keratinocytes and melanocytes causing mutations in the DNA. UV-A is the predominant UV radiation, which can penetrate until the dermis, resulting in fibroblast damage, collagen degradation, dysregulation of metalloproteinases, and photoaging processes [3]. However, in cosmeceutical terms UVB rays are more directly linked to skin cancer, while UVA rays are more linked to premature aging.

Skin cancer is among the most common cancers worldwide, with increasing incidence and mortality rates, mostly in regions with white-skinned population [5]. In response to this, public and private organizations have initiate prevention and education campaigns, promoting early detection skin cancer and photoprotection

habits, e.g. reduce sun exposure during central hours of the day, wear appropriate clothes and hats, use sunglasses or apply sunscreens (SPF > 30). Recent evidence indicates that UV radiation is not the only factor responsible for skin cancer and other skin issues. Other environmental and lifestyle factors, known as exposome, also play an important role. These factors include climate change, pollution, smoking, stress or poor nutrition [2] [6] [7] [8] (Vineis et al., 2020).

Sunscreens are essential for preventing the harmful effects of UV radiation on health. These formulations include UV filters, typically classified as chemical or physical. However, this classification is often misunderstood. The US Food and Drug Administration (FDA) clarifies that all UV filters, including mineral filters, are chemical substances because they absorb UV photons, particularly in their nanoscale forms. Thus, mineral filters are not exclusively physical UV filters [9]. Chemical filters, which primarily consist of organic molecules such as para-aminobenzoic acid derivatives, benzophenones, salicylates, and cinnamates, can release absorbed UV energy as heat, emit radiation at longer wavelengths, or undergo molecular changes. These filters are often combined to achieve broad-spectrum protection, although their interaction may sometimes alter the SPF factor [2]. Physical filters, including zinc oxide (ZnO) and titanium dioxide (TiO_2), reflect or scatter UV radiation. Unlike organic filters, they are non-toxic and hypoallergenic but may present cosmetic and rheological challenges [9]. However, several of them are being eliminated of sunscreen formulations due to their unfavorable impacts on the environment, humans or marine ecosystems [2]. For these reasons, regulatory marks such as Scientific Committee on Consumer Safety (SCCS) and consumer trends are looking for new formulations that are environmentally friendly and non-harmful to life's ecosystem and should be brought to the market.

Beyond its capacity to absorb UV radiation, biological and natural UV filters have recently attracted a lot of interest from companies and health authorities because of their numerous benefits for skin. These compounds have anti-inflammatory, anti-aging, and antioxidant properties, among other important benefits. In addition, they are thermostable, photostable, and environmentally benign, which makes them a viable and efficient choice for sun protection. [10][11][12].

Saffron has gained significant interest as an ingredient in cosmetic formulations due to its potent anti-inflammatory and antioxidant properties, which have been extensively demonstrated through both in vitro and in vivo studies. The

stigma of saffron is particularly rich in a diverse array of bioactive compounds, including various crocins, picrocrocin, and carotenoids (Kothari et al., 2021). [13]. These compounds exhibit a range of biological activities, with crocins and picrocrocin playing key roles in modulating the redox balance of biological systems, thereby underpinning their antioxidant and anti-inflammatory effects [14]. The therapeutic potential of saffron has been explored in the treatment of numerous skin conditions, including erysipelas, acne, purpura, wrinkles, and eczema, further emphasizing its relevance in dermatological and cosmetic applications [15]. The widespread use of saffron and its apocarotenoids remains significantly limited due to their high production costs, which have earned saffron the nickname "red gold." To overcome this economic barrier, Ahrazem et al. (2022) developed "Tomafran," a genetically modified tomato variant designed to produce crocins and picrocrocin [16]. This breakthrough was achieved by integrating the saffron biosynthetic pathway into tomatoes, utilizing fruit-specific promoters to drive compound production in a tissue-specific manner. This innovation offers a promising and cost-effective platform for producing these high-value saffron metabolites, enabling their broader application in various industries. Moreover, the Tomafran fruit and its extract are rich in bioactive substances, including polyphenols, carotenoids, and crocins, further enhancing its potential for nutraceutical, pharmaceutical, and cosmetic applications [17] [18]..

One of the most significant challenges in the cosmetic industry is the limited efficacy of active ingredients, often attributed to inadequate skin penetration, instability, or insufficient contact with the target site. To overcome these limitations, various strategies have been developed, including chemical modifications and nanotechnology-based encapsulation techniques. The term "nanocosmetic" has emerged to describe the incorporation of nanomaterials or nanoformulations into cosmetic products, aiming to enhance their performance. These nanotechnology-driven approaches employ a diverse array of delivery systems for active ingredients, such as dendrimers, lipid-based nanocarriers, nanocapsules, polymeric nanoparticles, and metal nanoparticles. Each of these systems is specifically designed to improve the stability, bioavailability, and targeted delivery of active compounds, thereby maximizing the efficacy and benefits of cosmetic products .[19] [20]. Liposomes are excellent candidates for skin application formulations because their components, such as phosphatidylcholine or cholesterol, are biocompatible with the skin, do not

present toxicity, and also maintain a controlled release of the active compound, ensuring its protection against external degradation [21] [22] [23]. Liposomal vehicles form an occlusive barrier on the surface of the skin, providing moisture, therefore are highly recommended for use on dry skin, especially when there is overexposure to the sun and therefore UVR. Thus, formulations already available that thanks to this barrier property, products with aqueous active ingredients containing UV filters acquire greater resistance to water [24].

Given the well-documented advantages of liposomal formulations in industrial applications and commercialization, we encapsulated the Tomafran extract—rich in crocins, picrocrocin, and phenolic compounds—within liposomes.

The main objective was to develop a new liposomal formulation as well as to evaluate the antioxidant, anti-aging and natural UV filtering properties of the active ingredient. In addition, the encapsulation was designed to improve the stability of the Tomafran extract during storage without compromising its bioactive properties. This strategy aims to ensure that the extract retains its functional attributes over time, demonstrating the potential of liposomal systems to improve the preservation and efficacy of high-value botanical extracts.

2. Material and methods

2.1. Materials

L-α-phosphatidylcoline, cholesterol, chloroform, and the solvents used were purchased from Sigma-Aldrich (Madrid, España). DMEM low glucose medium (Gibco), FBS (Gibco), Penicillin/Streptomycin (Life Technologies), L-Glutamine (Gibco), Phosphate buffered saline (Gibco), Trypan Blue Solution (Bio-Rad), Trypsin-EDTA (Gibco), Trypan Blue Solution (Bio-Rad), Triton X-100 (Fisher), Tris base (Fisher), SDS (Sigma), MTT reagent [3-(4,5-Dimethylthiazol-2-yl)-2,5-Diphenyltetrazolium Bromide] (Invitrogen), dimethyl sulfoxide (DMSO, Sigma-Aldrich), and Intracellular ROS detection kit (Sigma Aldrich).

2.2. Tomafran extract preparation

The Tomafran extract was prepared following the method previously described in [25] with some modification. Briefly, the harvested fresh tomato fruits were washed

with sterile distilled water prior to frozen and freeze-drying process. Once freeze-dried, they were pulverized with a blender until a homogeneous powder was obtained. Then, extractions were made in three technical replicates from the obtained powder. First, extractions were performed with 50 % MeOH in water for the recovery of polar crocins, and the samples sonicated during 10min. Next, samples were centrifuged for 10 min at 12,000 g in a microcentrifuge, and the supernatant was recovered for crocin analysis by HPLC-DAD, lyophilized, and stored at 4 °C for further analysis.

2.3. Biochemical composition of extracts

2.3.1 HPLC crocin determination

To extract the crocins, the lyophilized material was ground up in a mill. 50 mL of 75% MeOH was used to extract 5g of each sample, which was then stirred for 30 minutes at 20°C, sonicated for 10 minutes in a water bath, and centrifuged to remove any remaining solids. After dissolving each extract in 1 mL of 75% MeOH, 20 µL were subjected to HPLC-DAD analysis as previously described [16]. All samples were analyzed in triplicate.

2.3.2 UV-visible spectra

Ultraviolet and visible spectra were determined by using a double beam spectrophotometer (UV-2600i, Shimadzu, Japan) in the range of 280 to 750nm using MeOH:H_20 as solvent.

2.3.3 Determination of phenolic compounds

Phenolic compounds were quantified according to the Folin-Ciocalteau method [26]. The extract (powder) was dissolved in H_2O:EtOH (1:1) at a concentration of 2mg mL^{-1}. For the reaction, 50 µL of the extract was mixed with 750 µl of distilled H_2O, 50ul of Folin-Ciocalteau reagent (Sigma-Aldrich) and 150 µl of 20% Na_2CO_3 in water. After 2h of incubation in refrigerator (4ºC) and darkness, absorbance was measured in a Multiskan (Thermo) at 750 nm. A standard curve was made with gallic acid.

2.3.4 Determination of flavonoids

Flavonoids were determined through the aluminium chloride colorimetric assay [27]. The powder extract was dissolved in H_2O:EtOH (1:1) at a concentration of 2 mg mL^{-1}. For the reaction, 50 μL of the extract were mixed with 150 μl of ethanol and 5 μL of aluminium chloride (2% in ethanol). After 1 hour of incubation, absorbance was measured in a microplate reader (Multiskan FC, Thermo) at 405 nm. Quercetin was used as standard.

2.4. Antioxidant capacity of the extracts

The antioxidant capacity was evaluated using three different methods, two of them based on the free radical scavenging activity (ABTS and DPPH) and the other based on the decoloration of the B-carotene.

The ABTS method was performed according to Re et al. (1999). The ABTS+- radical is generated by mixing 7 mM ABTS (2,2'-azino-bis (3- ethylbenzothiazoline-6-sulfonic acid) and 2.45 mM K2S2O8 in phosphate buffer (0.1M; pH 6.5). The mixture is kept for 12-16h at room temperature for complete formation of the ABTS+- radical. The ABTS+- radical was diluted to an initial absorbance of 0.75 ± 0.05 at 727 nm. For the reaction, 950 mL of diluted ABTS+- was mixed with 50 mL of the extract. Incubate for 8min in the dark and measure absorbance at 727 nm.

The DPPH method was performed according to Brand-Williams et al. [28]. A 150mM solution of DPPH in 80% methanol is prepared (should have initial absorbance at 517 nm of 0.8 ± 0.05). For the reaction 800 mL of DPPH is mixed with 200 mL of extract. The mixture is incubated for 15min in the dark and absorbance was measured at 517 nm.

For both cases, the % antioxidant capacity was calculated as follows: (Absini - Abs_fin)/Abs_ini, and a a standard line was made with Trolox (6-hydroxy-2,5,7,8-tetramethylchroman-2-carboxylic acid). The results are expressed as umol TE g-1 DE (Dry Extract).

The third assay, the β-carotene bleaching assay (BCBA) was performed as described Zubia et al. (2007). One mL of β-carotene (1 mg in 5 mL chloroform) was mixed with 25 μL of linoleic acid and 200 mg of tween-20. The chloroform was evaporated under vacuum at 40ºC and the residue were vigorously mix with 50 mL of distilled water to form a emulsion. For the reaction, 50 μL of the extracts were mixed with 200 μL of the emulsion. After measure the initial absorbance at 450 nm

in a microplate reader (Multiskan FC, Thermo), samples were incubated at 50ºC and measured the absorbance each 3 min during 3h.

2.5. In vitro evaluation of tomafran extract as cosmeceutical agent

2.5.1 Cell viability (MTT) assay

The optimal dosage of tomafran extract was evaluated for the next cell experiment conducting a MTT assay. It is based on the ability of metabolically active cells to transform a water soluble dye (3-(4-5dimetylthiazol-2-yl)2-5dipheyltretazolium bromide) into an insoluble formazan Briefly, cell numbers and viability were determined using Trypan-Blue staining and counting in a Bürker chamber under the microscope. For the MTT viability assay, human fibroblasts were cultured overnight at a 10.000 cells/well density in a 96 well plate in supplemented growth medium. After 24h, the culture medium was replaced with fresh medium containing TF-Extract at 8 different concentrations (3, 1, 0.3, 0.1, 0.03, 0.01, 0.003 and 0.001 %). After 24 h of incubation, the medium was removed, and MTT solution was added to each well. Plates were incubated at 37ºC for 3 h. The MTT reagent was removed and 100 % DMSO was added to each well to solubilize formazan crystals. The absorbance was then measured at 550 nm and 620 nm as a reference on a scanning multi-well spectrophotometer.

2.5.2 AGEs quantification

Human fibroblasts were treated with TF-Extract at 0.1 % and 0.01 % for 24 h. After the incubation period, the cells were exposed to UVB irradiation (Luzchem Irradiator LZC-420 with UVB lamps 1.8 kJm^{-2}). Non-irradiated controls were incubated at 37ºC during this time. After irradiation, samples were processed for Advanced Glycation End-products (AGE) quantification in the cell lysates. AGE levels were quantified with a specific ELISA kit following the manufacturer's instructions. ELISA standards were used to generate a standard curve and interpolate the sample values. In parallel, cell viability was quantified using the MTT assay to normalize AGE levels to the number of live cells due to UVB-induced cytotoxicity.

2.5.3 ROS UVA quantification

Human keratinocytes were cultured overnight at a 10.000 cells/well density in a black 96-well plate in growth media. After 24 h, the culture media was removed

and replaced by new culture medium supplied with TF-Extract at 0.01 % and 0.001 % concentrations. After an additional 24 h of incubation, PBS and ROS master mix (2',7'-dichlorofluorescein diacetate (DCFH-DA; Molecular Probes, Leiden, Netherlands)) were added to all cultured wells and cells were exposed to UVA radiation at 5 h at an intensity of 20 J/cm^2 (Luzchem Irradiator LZC-420 with UVA lamps) [29][30]. Non-irradiated controls were incubated at 37ºC during this time in the dark. 2 hours after ROS master mix addition to cells, ROS levels were measured in all samples. Intracellular ROS react with a fluorogenic sensor localized in the cytoplasm, resulting in a fluorescent product whose appearance is proportional to ROS levels. Fluorescence quantification was measured at λex =490 nm/ λem =525 nm. In parallel, cell viability was quantified through MTT assay to normalize ROS levels to the number of live cells due to UVA-induced cytotoxicity.

2.6.Formulation and characterization of empty and TF-Liposomes

Liposomes were prepared according to the film hydration method described in [31] with some modifications. Briefly, 90 mg of L-α-phosphatidylcholine and 10 mg of cholesterol were dissolved in 4 mL of chloroform, after which the solvent was evaporated at 40°C using a rotary evaporator under vacuum. The lipid film formed in the round-bottomed flask was rehydrated by adding 10 mL of PBS and left under stirring for 30 min in the rotavapor without vacuum, so that the lipids formed lipid vesicles of different sizes. Next, a liposome extruder kit was used to reduce and homogenize the size of the formed liposomes. The kit consists of a holder, two 1 mL Hamilton needles, and 0.1 µm membranes (Avanti Polar Lipids; Alabaster, Alabama). Each milliliter of suspension was passed through the system 30 times to optimize the PDI of the nanoparticles.

For the encapsulation of the crocin-rich tomato extract, the same method was used as for the empty liposomes but the crocin-rich extract of Tomafran was added. Before rehydrating the lipid film formed in the flask, 200 mg of the extract was dissolved in 10 mL PBS. Thus, when lipid vesicles are formed, the extract dissolved in the aqueous phase is encapsulated. The nanoparticle suspension was passed through the extruder 30 times.

2.6.1. Liposomes characterization

The characterization of liposomes (particle size, zeta potential and polydispersity index (PDI)) was determined by photon correlation spectroscopy through Dynamic light scattering (DLS) using a Zetasizer (3000HSM Malvern Ltd, IESMAT, Spain) with the following specifications: liposome refractive index (IR) of 1.450, absorption index 0.010, and water solvent RI: 1.33, with a viscosity of 0.8872 cP. Measurements were performed in triplicate.

2.6.2. Morphology studies

A Jeol JEM 210 TEM microscope was used to obtain high resolution electron microscope images, operating at 200 kV and equipped with an Oxford Link EDS detector. The resulting images were analyzed using Digital Micrograph™ software from Gatan.

2.6.3 Encapsulation efficiency and loading capacity.

Encapsulation efficiency was calculated using the crocin concentration as a standard. Lipid membranes are disorganised and dehydrated by ethanol, which is how the liposomes are destroyed when 9 ml EtOH were added. The liposomes were filtered through 0.2mm and injected into HPLC with a Zorbax Sb C8 3.5um 150 x 4.6mm column (Agilent). Mobile phases contained A) methanol / ammonium acetate buffer (80:20, pH 7.2, 0.5M), B) acetonitrile / H_2O (90:10), and C) ethyl acetate, and were used with the gradient described in Gheysen et al [32].

The loading capacity (LC) and encapsulation efficiency (EE) of the extract were calculated according to the following equations:

EE % = (weight of encapsulated crocin (mg)) / (weight of crocin feeding (mg)) × 100%

LC % = (weight of encapsulated crocin (mg)) / (weight of total (crocin encapsulated + scaffold weight) (mg)) × 100%

2.6.4 Stability after storage

Particle size, zeta potential and polydispersity index were measured using suspension samples by dynamic light scattering (DLS) during storage at 4 °C for 15 and 30 days.

2.6.5 *In vitro release study of Tomafran-liposomes*

1 mL of liposomes was sealed in a dialysis membrane (molecular weight cut off 3500 Da) and suspended in 10 mL of phosphate-buffered saline at optimum pH in CPs (pH 6) with continuous stirring at 200 rpm to ensure homogeneity. At certain intervals of incubation time at 37 °C, 5 mL of release medium was removed to evaluate the amount of released terpene and replaced with 5 mL of fresh medium. The released Tomafran was evaluated using the amount of crocin as a reference with the conditions mentioned in section 2.8.

2.7 *Determination of Sun protection factor*

The extract (powder) was added to a base cream at 5, 10 and 15%. Liposomes were added to the base cream at 10 and 20%. The protocol described by Pissavini et al. [33], ISO 24443:2012 was used to determine the values of SPF (sun protection factor) with the spectrum of erythema action, UVAPF (UV-A protection factor) with the spectrum of action of persistent skin pigmentation and protection factors against other biological effects (BEPFs: Biological effective protection factors; e.g. elastosis, photoaging, photocarcinogenesis, immunosuppression and singlet oxygen formation) according to de la Coba et al [34].The creams were spread on PMMA (polymethylmethacrylate; 5cm x 5cm; 6mm roughness) plates at a concentration of 1.3mg cm^{-2} (total of 32.5mg across the plate). Transmittance was measured across the plates using a spectrophotometer (UV-2600i, Shimadzu) with an integrating sphere (ISR-2600plus). Using the following formula, the different photoprotection factors were calculated.

$$\text{PPFs} = \frac{\int_{\lambda=290}^{\lambda=400} Act.\ sp(\lambda) \cdot I(\lambda) \cdot d(\lambda)}{\int_{\lambda=290}^{\lambda=400} Act.\ sp(\lambda) \cdot I(\lambda) \cdot T(\lambda) \cdot d(\lambda)}$$

where,

PPFs = Photoprotection factors

Act. Sp = different action spectra

I = Irradiance of a sunny day at midday in summer of Malaga

D = wavelength step

T = Transmittance

2.8 *Photostability of extracts and liposomes*

The extracts were dissolved in water at a concentration of 2 mg mL^{-1} and the liposomes were diluted 5-fold. Both the extract and liposome were irradiated with a set off 3 Q-panel 340 lamps (Q-Lab, USA) for 30, 60 and 120 min corresponding to UVR doses of 47.3, 94.6 and 189.3 kJ m^{-2} being UVB and UVA. A thermoblock (IKA) was used for thermostability. The extracts and liposomes were maintained for 2h at 45, 60 and 80ºC. Subsequently, the amount of phenolic compounds, antioxidant capacity by ABTS and absorption spectra (280-750nm) were measured again. For liposomes, only the absorption spectrum was measured.

2.9 Anti-inflammatory properties of TF-liposomes in Cell Culture Model

Raw 264.7 cells (ATCC No TIB-71), were subcultured at 1.50×10 5 cells/cm 2 in DMEM medium (Lonza) supplemented with 10% FBS, 2 mM L-glutamine and 100 U/mL penicillin–streptomycin, cultures were treated with 25 µg/mL protein from liposomes, and 25 µg/mL and 50 µg/mL liposomes with encapsulated tomato extract, and incubated overnight in complete DMEM supplemented with 5% FBS, preceding activation with 150 ng/mL LPS from Salmonella typhimurium (Sigma-Aldrich).

RNA Isolation and Quantitative Real-Time Polymerase Chain Reaction (qPCR)

Real-time reverse transcriptional polymerase chain reaction was performed as follows. Total cellular RNA was isolated from treated and control cells with TRIzol reagent (Invitrogen). The concentrations were evaluated in a ND-1000 (NanoDrop) spectrophotometer. cDNA synthesis was performed using 1 µg of total RNA with the RevertAidH Minus First Strand cDNA Synthesis (Thermo Scientific), following manufacturer´s recommendations. Afterwards, Real-time PCR was performed with SYBR® Premix (Applied Biosystems™). Analysis was performed on Light Cycler 96 Real-Time PCR System (Applied Biosystems™). Specific oligonucleotides were designed with the PrimerQuest SM computer program (Integrated DNA technologies, Inc.Coralville IA, USA) The housekeeping gene mouse riboprotein P0 was used for normalization. The primers used in this study are shown in Table 1.

Table 1.Oligonucleotides used for PCR.

Gene	Forward Primer	Reverse Primer
P0	5′-GAATCGCTCCTGCAGCAAAG-3′	5′-CCAGGGTCTCATCCGCATT-3′
IL6	5′-CCACGGCCTTCCCTACTTC-3’	5′-TTGGGAGTGGTATCCTCTGTGA-3’
IFN-β	5′ AAGAGTTACACTGCCTTTGCCATC 3′	5′ CACTGTCTGCTGGTGGAGTTCATC 3′
IL12	5’-ACGAGAGTTGCCTGGCTACTAG-3’	5’-CCTCATAGATGCTACCAAGGCAC-3’

2.14 Statistical analysis

The obtained data were statistically analyzed using one-way ANOVA and Dunnet's Multiple Comparisons test with the statistical software GraphPad Prism version 5.0.0 for Windows, GraphPad Software, San Diego, California USA. Differences were tested on < 0.05 (95% probability level)

The MTT assay in the case of human fibroblasts was set with 8 replicates per condition and 16 for control, and the AGEs quantification assay was set with 4 replicates per condition. Data outliers were identified using the ROUT method (Q = 5 %) and excluded from the analysis if found. Raw data were statistically analyzed using ordinary one-way ANOVA test and Dunnet’s post hoc multiple comparison test. Statistical significance was set at $p < 0.05$, 95 % of confidence interval. Bars in the charts represent the mean value for each condition and error bars indicate the standard error of the mean (SEM) for each group of values. The MTT assay for human keratinocytes was set with 8 replicates per condition and 16 for control, and the ROS quantification assay was set with 4 replicates per condition. Data outliers were identified using the ROUT method (Q = 5 %) and excluded from the analysis if found. Raw data were statistically analyzed by means Unpaired t-test or ordinary one-way ANOVA test and Dunnet’s post hoc multiple comparisons test. Statistical significance was set at $p < 0.05$, 95 % of confidence interval. Bars in the charts represent the mean value for each condition and error bars indicate the standard error of the mean (SEM) for each group of values.

3 Results and discussion

3.1. Metabolite determination and antioxidant activity of Tomafran extract

Tomafran is a genetically modified tomato variant engineered to harbor the biosynthetic pathway for producing crocins and picrocrocin, compounds naturally found in saffron stigmas. In this study, the extract derived from Tomafran was characterized, and its bioactivities, particularly antioxidant capacity and UV photoprotection, were analyzed. For comparative purposes, extracts from conventional tomatoes and saffron stigmas were also characterized under similar conditions.

The HPLC analysis of tomato, saffron, and Tomafran extracts were previously performed in earlier studies [16][25]. A maximum amount of 5-6 mg of crocin g^{-1} DE (dried extract) of tomafran was obtained. Figure 1 shown the UV-Vis spectra of the extracts. Saffron spectrum highlight among tomato or Tomafran spectra, exhibiting the characteristic crocin absorption peak, ranging from 380 to 500nm. Tomato extract present a high absorption in the UV region, specifically between 280 and 350 nm. Tomafran extract also demonstrated absorption in the crocin region indicating the presence of this compound.

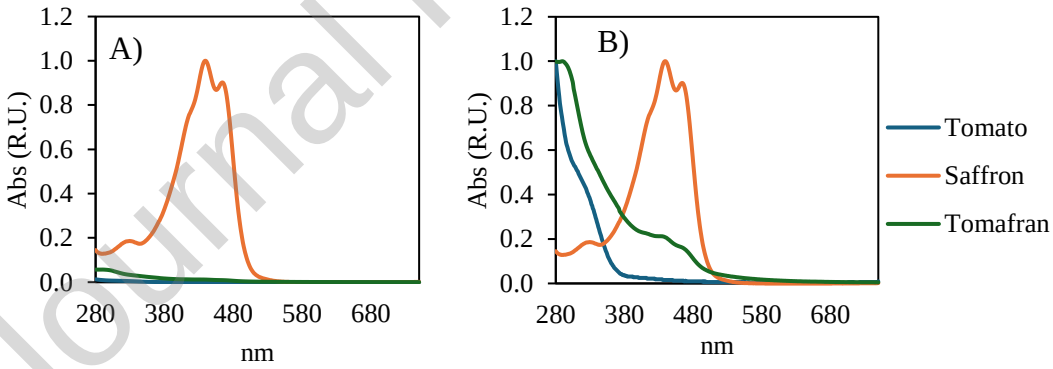

Figure 1. UV-visible spectra of tomato, saffron and Tomafran extracts. A) Values were normalized with respect to the maximum of the three of them; B) Values were normalized respect to the maximum of each one.

Figure 2 shown the concentration of total phenolic compounds (TPC) and total flavonoids (TF). Saffron presents the highest content of both of them, the content of phenols is 58.60 ± 5.37 mg g^{-1} DE and the content of flavonoids 39.41 ± 11.81 mg g^{-1} DE. Tomato presents much lower phenolic compounds (4.38 ± 0.60 mg g^{-1} DE), and no flavonoids were detected. Tomafran present 15.63 ± 2.69 mg g^{-1} DE of phenols and 4.75 ± 0.43 mg g^{-1} DE of flavonoids.

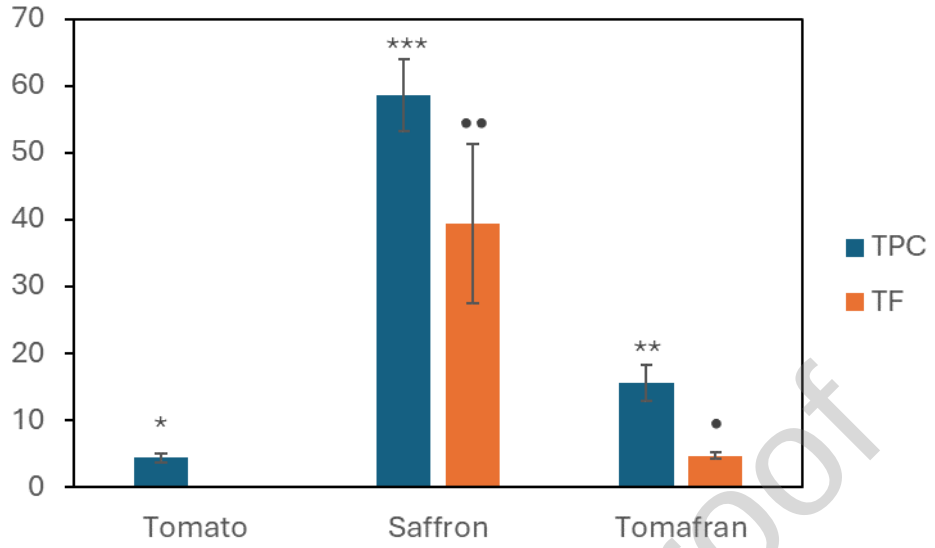

Figure 2. Total phenolic compounds (TPC) and total flavonoids (TF) concentration of tomato, saffron and Tomafran extract. Asterisk (*) indicate signficiant differences among extract of total phenolic compounds (ANOVA, Tukey post hoc, p> 0.05) and dot (•) indicate significant differences among extracts of flavonoids (Student t-test, p> 0.05).

The antioxidant capacity through two different free radical scavenging activity methods is observed in table 2. The results are expressed as µmol TE g^{-1} DE and as half maximal effective concentration (EC50; mg DE mL^{-1}). Using the ABTS methodology, the antioxidant capacity of Tomafran extract was approximately double that of unmodified tomato extract but remained lower than that of saffron extract. Specifically, Tomafran demonstrated an antioxidant capacity of 76.93 ± 8.15 µmol TE/g ($p < 0.05$), compared to 216.98 ± 21.38 µmol TE/g for saffron extract. In relation with the EC50, saffron showed values of 0.06 mg DE mL^{-1} and Tomafran values of 0.17 mg DE mL^{-1}. In contrast, in the DPPH assay showed more similar values among the three extracts, highliting the Tomafran extract (33.44 ± 4.92 µmol TE g^{-1} DE).

Table 2. Antioxidant capacity measured through ABTS and DPPH assay of tomato, saffron and tomafran. Values were calculated as umol TE g^{-1} DE and half maximal effective concentracion (EC50; mg DE mL-1). Asterisk (*) indicate signficiant differences among extract (ANOVA, Tukey post hoc, p> 0.05).

	ABTS		**DPPH**	
	µmol TE g^{-1} DE	**EC50 (mg DE mL^{-1})**	**µmol TE g^{-1} DE**	**EC50 (mg DE mL^{-1})**

Tomato	35.88 ± 3.68	0.40	21.83 ± 4.73	0.96
Saffron	216.98 ± 21.38	0.06	21.43 ± 5.14	0.86
Tomafran	76.93 ± 8.15	0.17	33.44 ± 4.92	0.56

Antioxidant capacity was also measured through the βcarotene bleaching assay (BCBA). In contrast to the ABTS and DPPH assay, this method did not shown a linear response (Figure 3). For example, the concentration of 0.1ug mL^{-1} showed values of 6.8, 39.2 and 32% of decoloration of the β-carotene in tomato, saffron and Tomafra, respectively. As in the case of the DPPH, similar values were obtained between saffron and Tomafran.

A)

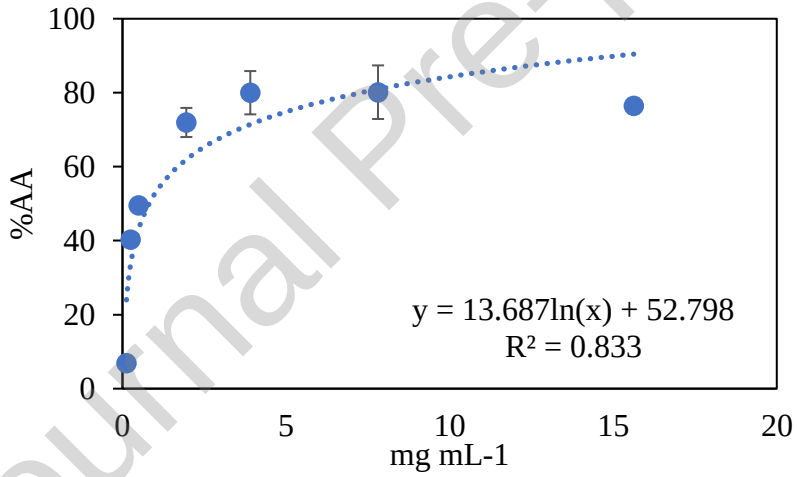

B)

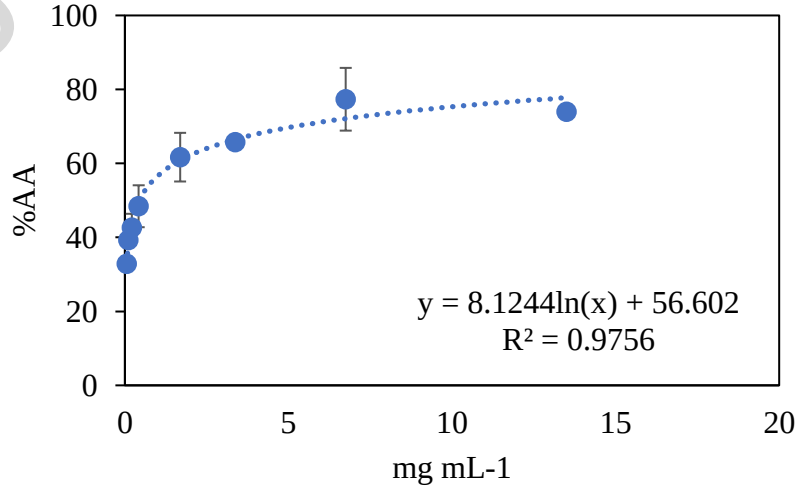

C)

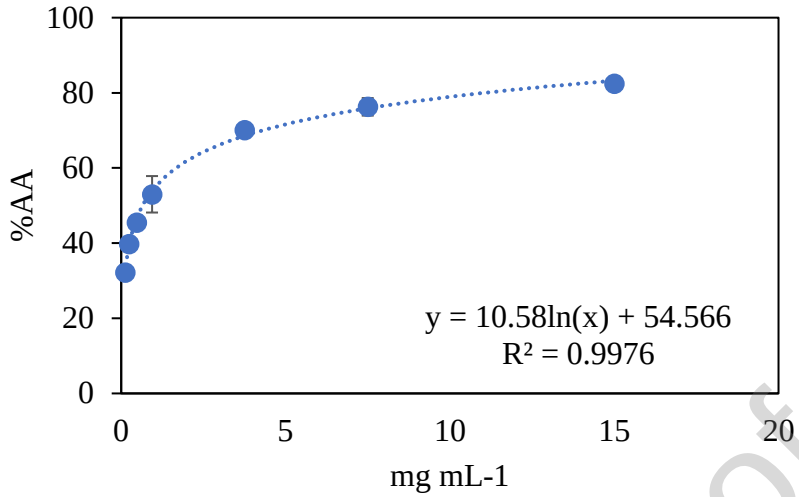

Figure 3. Antioxidant capacity measured through the β-carotene bleaching assay I Tomato (A),Saffron (B) and Tomafran (C) .

The showed results are in the range of other studies. Belyagoubi et al. (2021) analyzed Algerian saffron and observed 97.9 ± 10.5 mg g-1 DW of phenols and 5.9 ± 0.0 mg g-1 DW of flavonoids. However, Bellachioma et al. (2022) obtained 20 ± 3 mg g-1 of phenols and 2.4 ± 0.2 mg g-1 of flavonoids in saffron from Italy. In relation with the antioxidant capacity, Belachioma obtained much higher values, an EC50 of 28ug mL using the DPPH, whereas other studies showed a very low antioxidant capacity in the saffron stigma (Lahmass et al., 2017; Belyagoubi et al., 2021)

On the other hand, some plants with potential application in photoprotection such as pomegranate or coffee exhibit higher or similar content of these compounds and bioactivities. Pomegranate peel contains between 161 and 240 mg g-1 of phenols (Rosas-Burgos et al. 2017), while green coffee beans were in the range of 21.8 – 43.6 mg g-1 of phenols and 3.3-6.2mg g-1 of flavonoids (Mehari et al. 2020).

3.1 Cell viability (MTT assay) of human fibroblasts and keratinocytes.

The results showed that treatment with TF-Extract reduced cell viability at all concentrations tested, with the exception of 0.001%. Following the OECD standards for cell culture toxicity studies, which prescribe a 25% margin of safety, we defined a lower nontoxic threshold to determine the optimal working dosages for subsequent analyses. Based on this, the selected working concentrations for TF-Extract were 0.1 % and 0.01 %. Graphical representation of the results showing normalized cell viability after treatment of human fibroblasts cells with TF-Extract, compared to the

non-treated control. Data are presented as mean ± standard error of the median (SEM). Statistical significance is depicted as *** for $p < 0.001$, **** for $p < 0.0001$.

Results obtained in this assay using crocin-rich transgenic tomato extract, at concentrations of 0.001%, showed higher cell viability rates than other viability assays using saffron extract . This is demonstrated by the fact that the concentrations set at 0.01%-0.001% with 4.84 - 48.4 µg crocin/mL show a better trend in cell viability, whereas in J. Xiong's work, cell viability is limited to concentrations of 5-200 µg /mL of saffron extract, which is equivalent to a range of 0.455-18.2 µg crocin/mL. These results showing higher cell viability at higher crocin concentrations may be due to the synergic effect of other compounds, mostly antioxidants, present in the transgenic tomato extract [35].

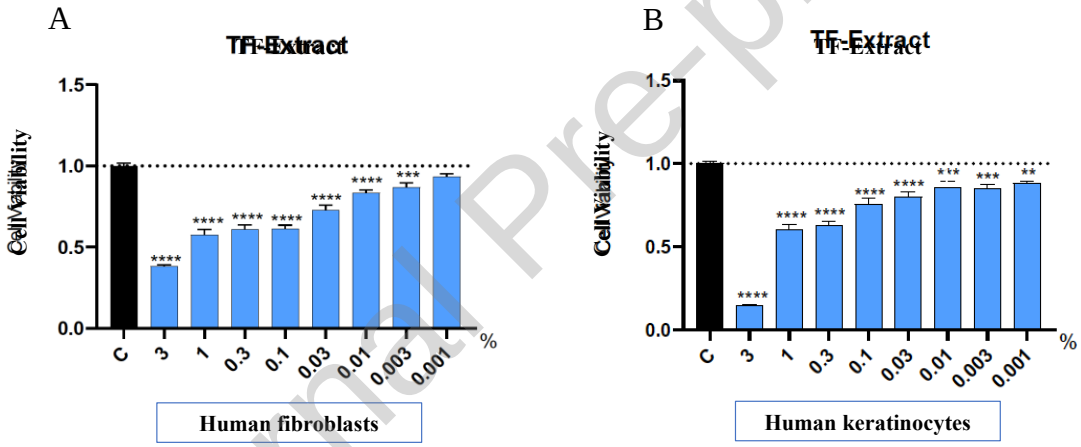

Fig. 4 Viability of human fibroblasts (A) and human keratinoytes (B) viability under different concentration of tomafran extracts.

3.2 AGEs quantification

AGEs (advanced glycation end products) represent a pathophysiological response associated with inflammation, oxidative stress, ageing, metabolic disorders and both dermatological and cardiovascular diseases. Their action mechanism at molecular level is based on their interaction with their transmembrane receptors, which further enhances the inflammatory signalling pathway and release of pro-inflammatory cytokines (IL-1 β, IL-6), in addition to matrix metalloproteinase (MMP) production and collagen degradation, resulting in photo-ageing. These inflammatory signalling responses have also been demonstrated by studies linking intracellular formation of AGEs by UVB radiation. [36]. The abundance of AGEs in the samples was determined by comparing their absorbance with that of a known

AGE-BSA standard curve (Fig. 5). The obtained raw data on the levels of AGEs were normalized to the cell viability quantified through the MTT assay.Bar graph representing cell viability (left) and AGEs levels related to cell viability (right) after treatment with TF-Extract for 24 h in human fibroblasts subjected to the UVB irradiation protocol. Data are presented as mean ± standard error of the median (SEM). * Represents statistical significance with p-value < 0.05, ** for p-value < 0.01 and *** for p-value < 0.001. The study evaluated the protective effects of TF-Extract against UVB-induced protein glycation in human fibroblasts. Results showed that UVB radiation increased AGEs levels in human fibroblasts by 48.6 ± 14.1 %, compared with the non-irradiated control. On the other hand, treatment with TF-Extract significantly decreased UVB-induced AGEs levels by 45.8 ± 14.1 % when used at 0.1 %. In conclusion, our study shows that treatment with TF-Extract protects against UVB-induced protein glycation in human fibroblasts.

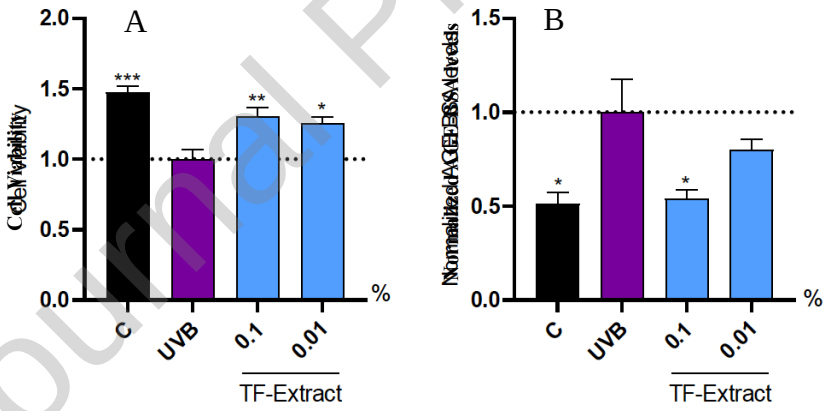

Fig. 5 Cell viability of human fibroblast (A) and normalized AGE-BSA levels (B) exposed to UVB radiation and the application of Tomafran extracts at 0.01 and 0.1%

3.3 ROS UVA quantification

The accumulation of ROS in the dermis stimulates the degradation of the extracellular matrix, causing cross-linking of the collagen-elastin network and

increasing the synthesis of matrix metalloproteinases (MMPs). All these, results in skin damage as deep wrinkles, dryness, roughness or irregular pigmentation, among others. Thus, the reduction of the ROS in the skin would prevent all these damages [37].

Results showed that UVA radiation significantly increased ROS levels in human keratinocytes by 19080 ± 697 % (190±7 folds), compared to the non-irradiated control, thus validating our experimental model to study the oxidative stress (Figure 6). When ROS basal levels were subtracted from all samples to assess UVA-induced oxidative stress protection, the results indicated that treatment with TF-Extract protected from UVA-induced ROS levels by 19.2 ± 7.3 % when used at 0.001 %. Graphical representation of the results showing cell viability after UVA exposure, UVA-induced ROS levels and UVA protection after treatment with TF-Extract after subtracting ROS basal levels. Data are presented as mean ± standard error of the median (SEM). Statistical significance is depicted as * for $p < 0.05$, **** for $p < 0.0001$.

The study evaluated the protective effects of TF-Extract against UVA radiation in human keratinocytes through ROS quantification. Results showed that UVA radiation significantly increased ROS levels in human keratinocytes by 19080 ± 697 %, compared to the non-irradiated control. When ROS basal levels were subtracted from all samples to assess UVA-induced oxidative stress protection, the results indicated that treatment with TF-Extract protected from UVA-induced ROS levels by 19.2 ± 7.3 % when used at 0.001 %. In conclusion, our study shows that treatment with TF-Extract protects against UVA-induced oxidative damage (ROS) in human keratinocytes.

The findings suggest that this novel biological filter has the potential to be integrated with other photoprotective agents to develop advanced sunscreens capable of mitigating the deleterious effects of reactive oxygen species (ROS) and preventing further damage induced by prolonged sun exposure.

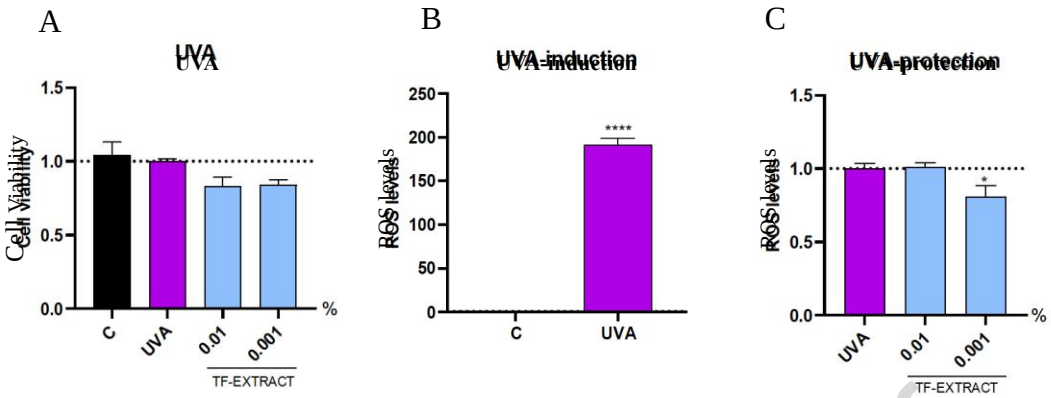

Fig. 6: Cell viability (A), induction of ROS levels of human keratinocytes exposed to UVA radiation (B) and under Tomafran extracts at 0.01 and 0.1%. (C)

3.4 Size, surface charge, PDI, EE and LE of Liposomes

Particle size and polydispersity index (PDI) measured with the DLS technique are commonly applied to determine the size of nanoparticles and the homogeneity of nanoformulations [38]. The results presented in *Table 3* shown that liposome formulations both empty and Tomafran-encapsulated exhibited correct size, homogeneity (PDI <0.3) and stability in aqueous media, since size values of 80.71 and 60.96, polydispersity indices of 0.17 and 0.06, Z-potential of -34.3 and -21.50 were obtained for empty liposomes and liposomes with Tomafran extract, respectively. Differences in size and PDI between blank liposomes and TF-liposomes could be attributed to the structure of the glycosylated crocins in the extract, being similar in structure to alkyl polyglycosides, which are a group of widely used non-ionic surfactants. This structure would consequently contribute to stabilize the formulation itself. Regarding other works involving liposome encapsulation for this type of compounds, similar results were obtained, such as the study carried out by Liu and collaborators, in which they encapsulated both vitamin C and β-carotene. Their results showed a mean diameter of 220.20 nm, 246.63 nm and 252.67 nm, for unloaded liposomes, liposomes with β-carotene and liposomes with vitamin C plus β-carotene respectively, obtained by the ethanol injection method. The polydispersity index and Z-potential values were also quite close to our results, with values of 0.44 and -25.65 mV for unloaded liposomes, 0.41 and -25.17 for liposomes with β-carotene, and 0.30 and -26.33 mV for liposomes with vitamin C and β-carotene. [39]. Liposomes containing saffron extract were prepared in a different study using the

Ultra-Turrax homogenization technique followed by a high-pressure homogenizer. The results showed particle size, Zeta potential and polydispersity index of 282.47 nm, -29.4 mV and 0.59 PDI without any cycle of high-pressure homogenization, whereas the first cycle reduced the particle size to 98.60 nm, PDI to 0.39 and Zeta potential was practically unaffected (-27.63 mV) [17]**.**

Regarding encapsulation efficiency and knowing that 200 mg of extract used contains 4.84 mg of crocin/g of extract and that each milliliter of liposomes contains 156 µg of crocin, the encapsulation efficiency was calculated to be 16.12%.

Table 3. Measurements for average size, PDI, Z-potential for liposomes and liposomes-TF at 0, 15 and 30 days. Also included EE% and LE%.

Liposomes	Days	Average size (r.nm)	PDI	Z-potential (mV)	%EE	LE%
Un-loaded Liposomes	0	80.71 ±0.28	0.17 ± 0.02	−34.3 ± 2.8	-	-
	15	83.45 ± 0.61	0.22 ±0.01	−28.40 ± 0.74	-	-
	30	84.08 ± 0.16	0.342 ±0.02	10.65 ± 1.77	-	-
Liposomes-TF	0	60.96 ± 0.18	0.06 ± 0.00	−21.50 ± 0.85	16.12 ± 0.02	24.24 ± 0.02
	15	73.10 ± 2.06	0.25 ± 0.03	−27.35 ± 0.21	-	-
	30	63.13 ± 0.35	0.06 ± 0.03	−24.95 ± 4.17	-	-

3.5 Storage stability

Measurements were taken for size, homogeneity and stability in aqueous medium after 15 days of storage, showing no considerable differences in size and stability, with 83.45 nm, 0.22 and -28.40 mV for the unloaded liposomes and 73.10 nm, 0.25 and -27.35 mV for the Tomafran extract liposomes. One-month results demonstrated little variation in size for both unloaded liposomes (84.08 nm) and Tomafran liposomes (63.13 nm). However, PDI and Zeta potential values were affected for liposomes without extract, with an increasing trend in PDI value reaching 0.342 and a decline in stability in aqueous medium reaching 10.65 mV. This pattern was not observed for the liposomes with Tomafran extract, as its PDI value was still quite homogeneous, and its Zeta potential value was barely altered, standing at -24.95 mV. According to these results, it is possible to conclude that liposomes without extract are thermodynamically unstable, with a tendency to display aggregation

processes [40]. Moreover, the difference in size numerical values during storage may be due to self-assembly and reorganization of the liposomes themselves. Finally, successful stability results for TF liposomes could support the previously mentioned stability effect due to crocin´s structure, similar to alkyl polyglycoside groups. Another study evaluated the storage stability of liposomes containing safranal, concluding that there were no significant changes in liposome size for at least 3 months. [41].

3.6 Morphological characterization of Liposomes

TEM micrographs were performed to evaluate the morphological and external characteristics of nano-formulations (Fig.7). The liposomes exhibited a distinctly spheric morphology containing a clear water reservoir and unilamellar structure that was slightly affected by the aggregation of the liposomes in the microscopy sample, without showing ruptures. Their size was generally smaller than 100 nm with a narrow polydispersity, which corroborates the data obtained by DLS. Regarding the vesicle size, qualitative analysis from TEM images confirmed that the morphological structure and approximate size of the vesicles were preserved post-lyophilization. However, we acknowledged the presence of some aggregation, which is attributable to thermal stress during freezing. The dynamic light scattering (DLS) analysis showed that while the mean hydrodynamic diameter remained within acceptable variation, the PDI increased from 0.06 to 0.3, indicating greater heterogeneity post-lyophilization. The size of the liposomes remained unaffected after the lyophilization process, indicating enhanced storage stability and confirming that the liposomes retain their morphological integrity.

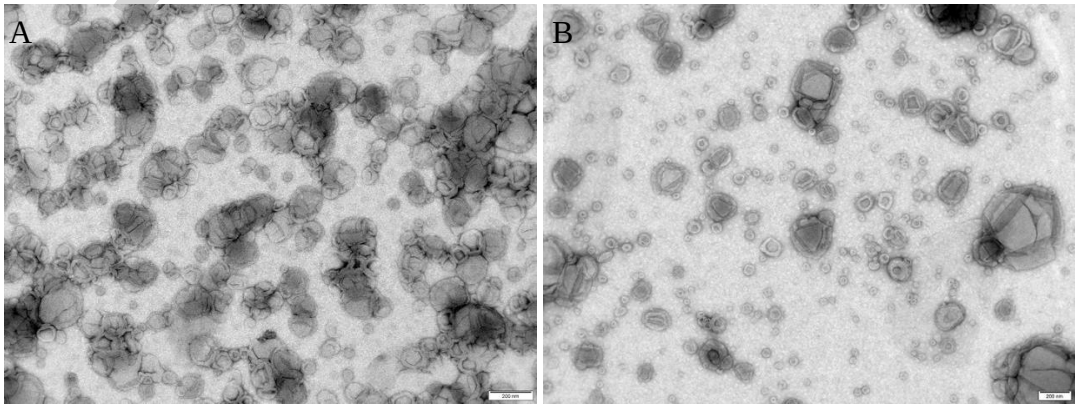

Figure 7. Liposomes before (A) and after (B) lyophilization, 60.96 (r.nm) PDI 0.06 and 85.72 (r.nm) PDI 0.3 respectively . Scale bar 200 nm

3.7 Release study

In vitro release studies of different nanomaterials or nanoformulations are a widely used strategy to better understand the physicochemical properties of the proposed nanomaterials by studying the kinetic mechanism involved in the drug release process [42]. Figure 8 shows a release profile in phosphate buffer solution of Tomafran extract encapsulated in Liposomes. Liposomes exhibit a biphasic release profile with an initial burst release phase achieving a total Tomafran release of 56.1% to the medium at 7 h. Subsequently, the release was governed by sustained release due to their diffusion mechanism with a very slight increase of release, achieving 57.5% of total release at 72 h confirming the very high stability of Liposomes in storage conditions. Biphasic release behavior is likely due to the molecular properties of the Tomafran extract. Its amphiphilic nature allows certain compounds to be weakly adsorbed onto or loosely associated with the lipid bilayer, resulting in a rapid initial release. In contrast, compounds encapsulated within the aqueous core are released more gradually, contributing to the sustained phase. This dual mechanism is now clearly discussed in the release study section. On the other hand, the biphasic release system is widely used in pharmaceutical and cosmetic systems with the aim of offering two different release stages of drug or active molecule dosage. The initial burst release is suitable to achieve a rapid effect of the active molecule; and the final phase to obtain a constant concentration of released compound avoiding the use of additional doses and the effect of adverse reaction dose related [43]. Due to the lipophilic/amphiphilic character of Tomafran extract molecules, compounds are able to remain both attached to the lipid membrane and encapsulated in the aqueous core. Other studies have concentrated on developing saffron extract liposomes that are more stable and resistant to harsh environments. Notably, Saroglu et al. developed nanoliposomes with a biphasic release pattern, attaining over 50% total saffron release after 27 hours of testing. This study demonstrates the potential of liposomal encapsulation in preserving the bioactivity and efficacy of saffron extracts in harsh environments. [17]. Mohammadi et al. encapsulated crocins in nanoliposomes to create a strategy for arthritis treatment that takes advantage of crocin's anti-inflammatory capabilities while also providing controlled release. Their investigation found that less than 40% of the crocin was released over a 168-hour period, indicating that this approach has the potential for long-term therapeutic effects. [44].

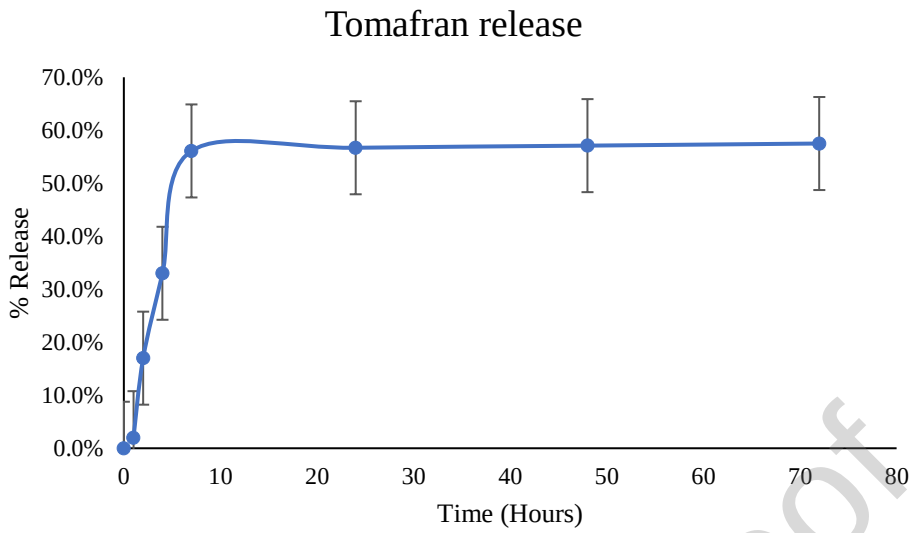

Figure 8. In vitro release study of Tomafran- Liposomes

3.8 Sun protection factor

Tomafran extract and liposomes containing the extract were added to a cosmetic formulation to measure their capacity to absorbed UV radiation through the calculation of different photoprotection factors. Tomafran extract added in different percentages increased the absorbance of the cream, although the photoprotection values increased to a very small extent, i.e. the cream with 15% of tomafran showed a SPF of 1.6 and a UVAPF of 1.2. The photoprotection of tomafran extracts on biological effects related to UVA radiation was lower than that related to UVB i.e the photoprotection increase related to the Base cream of 15% of UVA mediated effects was UVAPF (20.0%), Elastosis(20.3%), Photoaging (20.0% and singlet oxygen (21,8%) whereas of UVB mediated effects were SPF related to erythema (36.6%), photocarcinogenesis (46.3%) and immunosuppression (43,4%). This is probably because the polyphenols in the Tomafran extracts were more stable, and its contribution was much higher that due to crocins. However, when liposomes were added to the cream, no effect was observed. This may be because they are in a lower concentration or because the capsule protects them, so the effect of the extract is not evident until they are destroyed.

Other natural compounds have also shown low values. The addition of the algae Porphyra, that contain a high amount of mycosporine-like amino acids (MAAs) that present photoprotective properties, in a 25% only showed and SPF of 2.12 and UVAPF of 1.45 [45].

Table 4. SPF, UVAPF and photoprotection values against other biological effects: elastosis, photoaging, photocarcinogenesis, immunosuppression and singlet oxygen formation.

	Base	**5% TF**	**10% TF**	**15% TF**	**Lipos 10%**	**Lipos 20%**
SPF	1.20 ± 0.00	1.36 ± 0.02	1.46 ± 0.12	1.64 ± 0.12	1.21 ± 0.02	1.22 ± 0.01
UVAPF	1.01 ± 0.00	1.08 ± 0.00	1.12 ± 0.04	1.20 ± 0.05	1.04 ± 0.01	1.03 ± 0
Elastosis	1.03 ± 0.00	1.11 ± 0.01	1.16 ± 0.04	1.24 ± 0.05	1.06 ± 0.01	1.05 ± 0
Photoaging	1.01 ± 0.00	1.08 ± 0.00	1.13 ± 0.04	1.20 ± 0.05	1.04 ± 0.01	1.03 ± 0
Photocarcinogenesis	1.36 ± 0.01	1.57 ± 0.04	1.70 ± 0.20	1.99 ± 0.18	1.34 ± 0.03	1.39 ± 0.03
Immunosuppression	1.29 ± 0.01	1.49 ± 0.03	1.61 ± 0.17	1.85 ± 0.16	1.29 ± 0.03	1.32 ± 0.03
Singlet oxygen	1.01 ± 0.00	1.08 ± 0.00	1.14 ± 0.04	1.23 ± 0.05	1.04 ± 0.01	1.03 ± 0

3.9 Photostability of Tomafran extracts and liposomes-TF

Tomafran extract and its liposomal formulation were subjected to photostability and thermostability tests (Fig. 9). The phenolic content remained stable, unaffected by UV radiation or temperature. However, the antioxidant capacity (measured by ABTS assay) decreased in extracts exposed to UV radiation, particularly after 120 minutes. In the absorption spectrum, a noticeable decline in the crocin region absorption (380-500 nm) was observed after just 30 minutes of UV exposure. The maximal absorption in the tomafran extracts in the 460-480 nm interval, related to crocins, suffered a decline by both UV radiation and increased temperature (Fig, 10 A,B).

These results were expected as carotenoids are known to be labile compounds, that degrade easily under high temperature of light [46] [47].

In contrast, the liposomal formulation showed no significant changes in its absorption spectra under similar conditions (Fig 10 C,D)

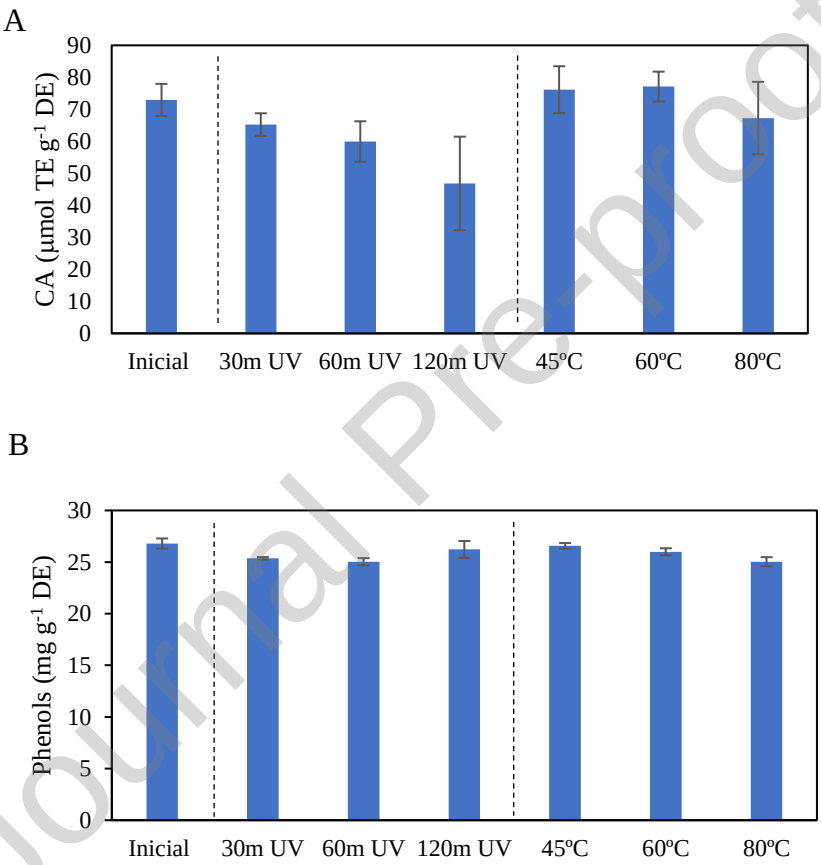

Figure 9. Tomafran extracts stability. A) Amount of phenolic compounds and B) Antioxidant capacity (ABTS).

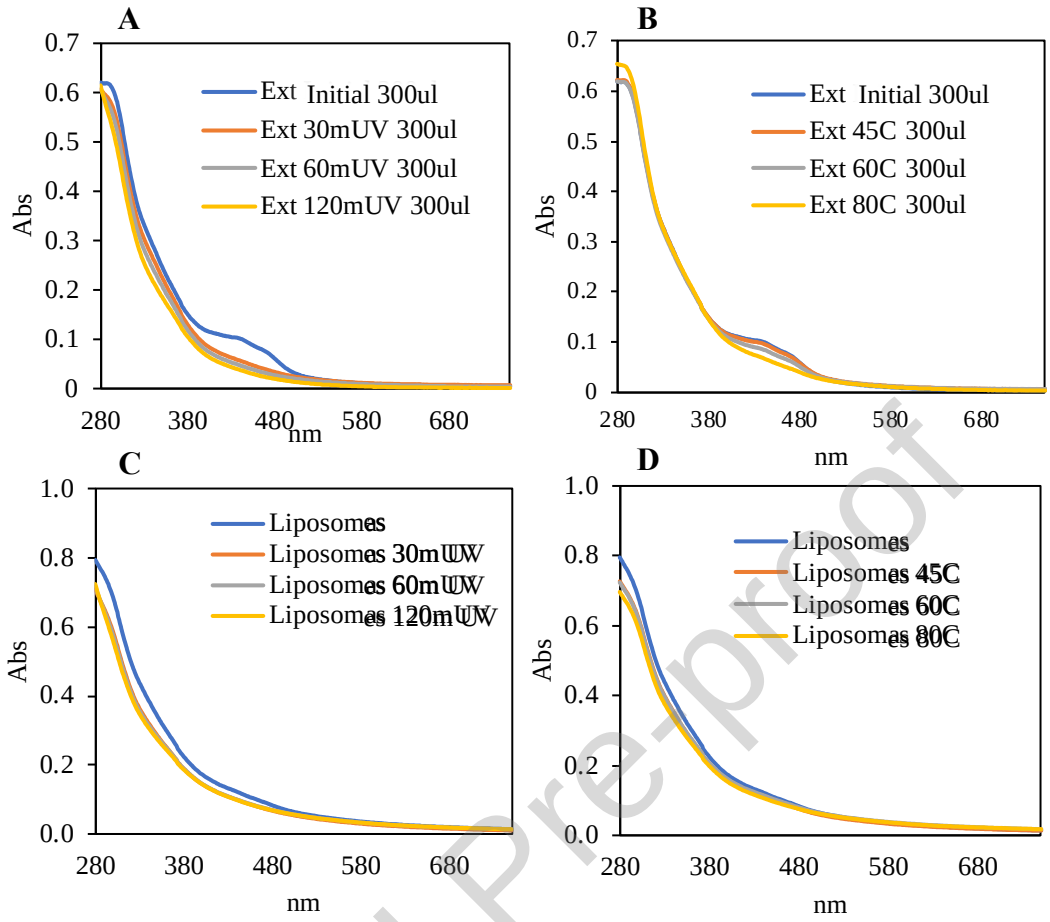

Figure 10. A-B Absorption spectra of tomafran extract subjected to photo- and thermostability. C-D Absorption spectra of liposomes containing tomafran extract subjected to photo- and thermostability.

3.10 Antiinflamatory properties of TF-liposomes

Finally, in order to evaluate the antiinflamatory powerfull of TF-LIposomes as antiinflamatory agent we determinate the evaluation of interferon and interleukine levels after treatment in widely used Raw 264.7 cells. The *figure 11* displayed the results of a*ssays* to determine the ani-inflammatory potential of liposome show a significant decrease in the mRNA expression levels of pro-inflammatory interleukins. Comparing liposome treatments with encapsulated extract against cells cultured with lipopolysaccharide (LPS) showed a decrease in mRNA levels of 96% for IL 6 and 93% for IL 12 at both concentrations (25 µg/mL and 50 µg/mL), no significant differences were shown between the different concentrations of liposome treatments with encapsulated extract. These treatments also resulted in a significant decrease in interferon beta mRNA levels by more than 90 %, compared to those treated with LPS alone. Other works with similar approaches through liposomal formulations propose the use of the liposome as a powerful tool to incorporate

molecules that serve as anti-inflammatory agents with the dual activity of the phospholipid bilayer of the liposome and its encapsulated molecule [48] [49]. On this line, the work developed by Mokdad et al. improve the antiinflamatory effect of Algerian thermal Waters encapsulating into liposomes achieving a very significative decreases in many proinflammatory markers such as TNFα and Interleukines [50]. Liposomal treatment with crocin-enriched tomato extract shows great anti-inflammatory potential and may open a line to future treatments of skin diseases caused by the pro-inflammatory effect such as that produced by skin sunburns.

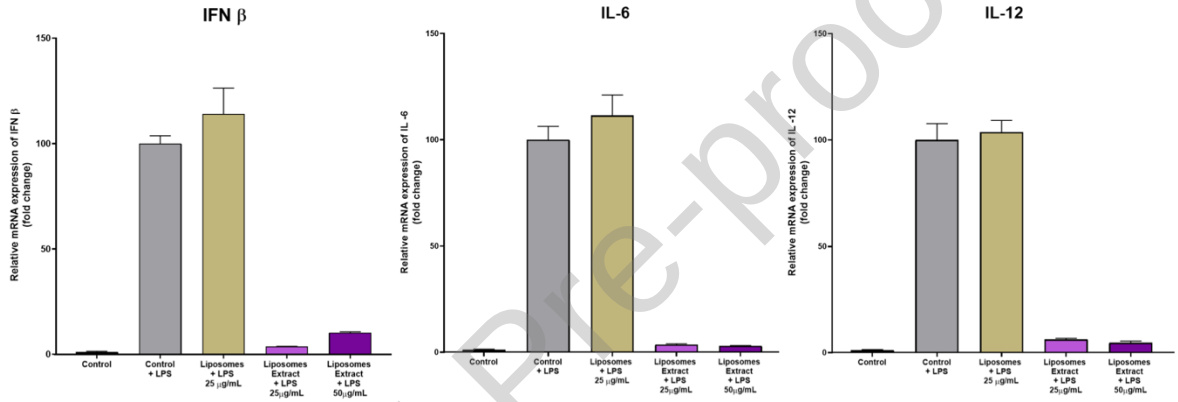

Figure 11. Proinflammatory levels of Raw 264.7 treated cells after LPS induction

4. Conclusion

The challenges associated with chemical synthesis compounds in conventional sunscreens have driven the exploration of alternative photoprotective agents with multifunctional properties. In this context, the photoprotective, antioxidant, and anti-inflammatory capacities of a genetically modified tomato extract rich in crocins, known as Tomafran, were evaluated. Tomafran represents a promising platform for the cost-effective production of crocins, significantly reducing production expenses while achieving competitive antioxidant properties. Tomafran extract exhibited protective effects against UVB-induced protein glycation in human fibroblasts, and significantly suppressed ROS generation in a UVA-induced oxidative stress assay. Furthermore, the extract was encapsulated in liposomes to enhance its stability and bioavailability. The particles present satisfactory characteristics, including particle size, polydispersity index, surface

charge, and storage stability, aligning with benchmarks established in similar nano-formulations. In terms of anti-inflammatory potential, the encapsulated extract demonstrated remarkable efficacy. A reduction in mRNA expression levels of proinflammatory cytokines was observed. These findings underscore the therapeutic potential of Tomafran liposomes not only as a photoprotective agent but also as a treatment for inflammatory skin conditions.

In conclusion, the encapsulation of Tomafran extract, rich in crocins, polyphenols, and other bioactive compounds, offers a promising approach for the development of multifunctional skincare products. Its combined photoprotective, antioxidant, and anti-inflammatory properties position it as a strong candidate for addressing skin burns, oxidative stress, and other dermatological conditions while also enhancing the economic feasibility of crocin-based applications.

Acknowledgment

MML was supported by the University of Castilla-La Mancha through a "Plan Propio" grant (2023-UNIVERS-11983).

Data availability

The data supporting our findings are available in the manuscript file or from the corresponding author upon request.

Bibliography

[1] K. J. Gromkowska-Kępka, A. Puścion-Jakubik, R. Markiewicz-Żukowska, and K. Socha, "The impact of ultraviolet radiation on skin photoaging — review of in vitro studies," *J. Cosmet. Dermatol.*, vol. 20, no. 11, pp. 3427–3431, 2021, doi: 10.1111/jocd.14033.

[2] O. P. Egambaram, S. Kesavan Pillai, and S. S. Ray, "Materials Science Challenges in Skin UV Protection: A Review," *Photochem. Photobiol.*, vol. 96, no. 4, pp. 779–797, 2020, doi: 10.1111/php.13208.

[3] R. M. Brand, P. Wipf, A. Durham, M. W. Epperly, J. S. Greenberger, and L. D. Falo, "Targeting mitochondrial oxidative stress to mitigate UV-induced skin damage," *Front. Pharmacol.*, vol. 9, no. AUG, pp. 1–10, 2018, doi:

10.3389/fphar.2018.00920.

[4] Y. Nakashima, S. Ohta, and A. M. Wolf, “Blue light-induced oxidative stress in live skin,” *Free Radic. Biol. Med.*, vol. 108, no. March, pp. 300–310, 2017, doi: 10.1016/j.freeradbiomed.2017.03.010.

[5] A. H. Roky *et al.*, “Overview of skin cancer types and prevalence rates across continents,” *Cancer Pathog. Ther.*, no. August, 2024, doi: 10.1016/j.cpt.2024.08.002.

[6] J. Krutmann, A. Bouloc, G. Sore, B. A. Bernard, and T. Passeron, “The skin aging exposome,” *J. Dermatol. Sci.*, vol. 85, no. 3, pp. 152–161, 2017, doi: 10.1016/j.jdermsci.2016.09.015.

[7] T. Gracia-Cazaña, S. González, C. Parrado, Juarranz, and Y. Gilaberte, “Influence of the Exposome on Skin Cancer,” *Actas Dermosifiliogr.*, vol. 111, no. 6, pp. 460–470, 2020, doi: 10.1016/j.ad.2020.04.008.

[8] T. Passeron, J. Krutmann, M. L. Andersen, R. Katta, and C. C. Zouboulis, “Clinical and biological impact of the exposome on the skin,” *J. Eur. Acad. Dermatology Venereol.*, vol. 34, no. S4, pp. 4–25, 2020, doi: 10.1111/jdv.16614.

[9] A. N. Geisler, E. Austin, J. Nguyen, I. Hamzavi, J. Jagdeo, and H. W. Lim, “Visible light. Part II: Photoprotection against visible and ultraviolet light,” *J. Am. Acad. Dermatol.*, vol. 84, no. 5, pp. 1233–1244, 2021, doi: 10.1016/j.jaad.2020.11.074.

[10] J. Aguilera, T. Gracia-Cazaña, and Y. Gilaberte, “New developments in sunscreens,” *Photochem. Photobiol. Sci.*, vol. 22, no. 10, pp. 2473–2482, 2023, doi: 10.1007/s43630-023-00453-x.

[11] L. Li, L. Chong, T. Huang, Y. Ma, Y. Li, and H. Ding, “Natural products and extracts from plants as natural UV filters for sunscreens: A review,” *Anim. Model. Exp. Med.*, vol. 6, no. 3, pp. 183–195, 2023, doi: 10.1002/ame2.12295.

[12] J. Vega *et al.*, “Isolation of Mycosporine-like Amino Acids from Red Macroalgae and a Marine Lichen by High-Performance Countercurrent Chromatography: A Strategy to Obtain Biological UV-Filters,” *Mar. Drugs*, vol. 21, no. 6, 2023, doi: 10.3390/md21060357.

[13] D. Kothari, R. Thakur, and R. Kumar, “Saffron (Crocus sativus L.): gold of the spices—a comprehensive review,” *Hortic. Environ. Biotechnol.*, vol. 62,

no. 5, pp. 661–677, 2021, doi: 10.1007/s13580-021-00349-8.

[14] M. Etxebeste-Mitxeltorena *et al.*, "Neuroprotective properties of exosomes and chitosan nanoparticles of Tomafran, a bioengineered tomato enriched in crocins," *Nat. Products Bioprospect.*, vol. 14, no. 1, 2024, doi: 10.1007/s13659-023-00425-9.

[15] Z. Mousavi and Z. Bathaie, "Historical uses of saffron: Identifying potential new avenues for modern research," *Avicenna J. Phytomedicine*, vol. 1, no. 2, pp. 57–66, 2011.

[16] O. Ahrazem *et al.*, "Engineering high levels of saffron apocarotenoids in tomato," *Hortic. Res.*, vol. 9, no. December 2021, pp. 1–13, 2022, doi: 10.1093/hr/uhac074.

[17] O. Saroglu, B. Atalı, R. M. Yıldırım, and A. Karadag, "Characterization of nanoliposomes loaded with saffron extract: in vitro digestion and release of crocin," *J. Food Meas. Charact.*, vol. 16, no. 6, pp. 4402–4415, 2022, doi: 10.1007/s11694-022-01526-8.

[18] L. Morote *et al.*, "A carotenoid cleavage dioxygenase 4 from Paulownia tomentosa determines visual and aroma signals in flowers," *Plant Sci.*, vol. 329, no. February, 2023, doi: 10.1016/j.plantsci.2023.111609.

[19] M. Mondéjar-López, A. J. López-Jimenez, J. C. García Martínez, O. Ahrazem, L. Gómez-Gómez, and E. Niza, "Comparative evaluation of carvacrol and eugenol chitosan nanoparticles as eco-friendly preservative agents in cosmetics," *Int. J. Biol. Macromol.*, vol. 206, no. February, pp. 288–297, 2022, doi: 10.1016/j.ijbiomac.2022.02.164.

[20] M. Mondéjar-lópez, A. J. López-jiménez, J. C. G. Martínez, O. Ahrazem, L. Gómez-gómez, and E. Niza, "Thymoquinone loaded chitosan nanoparticles as new ' eco - friendly ' preservative agent in cosmetic products," *Int. J. mol*, vol. 22, pp. 1–14, 2021.

[21] K. Barge, S. Tank, B. Parab, M. Nagarsenker, and S. Shidhaye, "Liposomal Cosmeceuticals as Skin Protectives and Curatives," *Indian J. Pharm. Educ. Res.*, vol. 58, no. 1, pp. 34–44, 2024, doi: 10.5530/ijper.58.1.4.

[22] A. Figueroa-Robles, M. Antunes-Ricardo, and D. Guajardo-Flores, "Encapsulation of phenolic compounds with liposomal improvement in the cosmetic industry," *Int. J. Pharm.*, vol. 593, no. November 2020, p. 120125, 2021, doi: 10.1016/j.ijpharm.2020.120125.

[23] S. K. Dubey, A. Dey, G. Singhvi, M. M. Pandey, V. Singh, and P. Kesharwani, "Emerging trends of nanotechnology in advanced cosmetics," *Colloids Surfaces B Biointerfaces*, vol. 214, no. December 2021, p. 112440, 2022, doi: 10.1016/j.colsurfb.2022.112440.

[24] V. Soni, S. Chandel, P. Jain, and S. Asati, *Role of liposomal drug-delivery system in cosmetics*. Elsevier Inc., 2016.

[25] L. Morote *et al.*, "Crocins-rich tomato extracts showed enhanced protective effects in vitro," *J. Funct. Foods*, vol. 101, no. November 2022, pp. 1–8, 2023, doi: 10.1016/j.jff.2023.105432.

[26] J. A. R. V. L. Singleton, "Colorimetry of Total Phenolics with Phosphomolybdic-Phosphotungstic Acid Reagents," *Am J Enol Vitic.*, vol. 16, no. no.3, pp. 144–158, 1965, doi: 10.5344/ajev.1965.16.3.144.

[27] J. Zacarías-Garcia, G. Carlos, J. V. Gil, J. L. Navarro, L. Zacarías, and M. J. Rodrigo, "Juices and By-Products of Red-Fleshed Sweet Oranges: Assessment of Bioactive and Nutritional Compounds," *Foods*, vol. 12, no. 2, pp. 1–26, 2023, doi: 10.3390/foods12020400.

[28] W. Brand-Williams, M. E. Cuvelier, and C. Berset, "Use of a free radical method to evaluate antioxidant activity," *LWT - Food Sci. Technol.*, vol. 28, no. 1, pp. 25–30, 1995, doi: 10.1016/S0023-6438(95)80008-5.

[29] A. Svobodová, A. Zdařilová, J. Mališková, H. Mikulková, D. Walterová, and J. Vostalová, "Attenuation of UVA-induced damage to human keratinocytes by silymarin," *J. Dermatol. Sci.*, vol. 46, no. 1, pp. 21–30, 2007, doi: 10.1016/j.jdermsci.2006.12.009.

[30] E. Tabolacci *et al.*, "Rutin Protects Fibroblasts from UVA Radiation through Stimulation of Nrf2 Pathway," *Antioxidants*, vol. 12, no. 4, 2023, doi: 10.3390/antiox12040820.

[31] Y. Yang, Y. Li, K. Goh, C. H. Tan, and R. Wang, "Liposomes-assisted fabrication of high performance thin film composite nanofiltration membrane," *J. Memb. Sci.*, vol. 620, no. August 2020, 2021, doi: 10.1016/j.memsci.2020.118833.

[32] L. Gheysen *et al.*, "Impact of Nannochloropsis sp. dosage form on the oxidative stability of n-3 LC-PUFA enriched tomato purees," *Food Chem.*, vol. 279, no. December 2018, pp. 389–400, 2019, doi: 10.1016/j.foodchem.2018.12.026.

[33] M. Pissavini *et al.*, "Validation of an in vitro sun protection factor (SPF) method in blinded ring-testing," *Int. J. Cosmet. Sci.*, vol. 40, no. 3, pp. 263–268, 2018, doi: 10.1111/ics.12459.

[34] F. de la Coba *et al.*, "UVA and UVB Photoprotective capabilities of topical formulations containing mycosporine-like amino acids (maas) through different biological effective protection factors (BEPFs)," *Mar. Drugs*, vol. 17, no. 1, 2019, doi: 10.3390/md17010055.

[35] J. Xiong, M. H. Grace, H. Kobayashi, and M. A. Lila, "Evaluation of saffron extract bioactivities relevant to skin resilience," *J. Herb. Med.*, vol. 37, no. October 2022, p. 100629, 2023, doi: 10.1016/j.hermed.2023.100629.

[36] R. Sultana, A. Parveen, M. C. Kang, S. M. Hong, and S. Y. Kim, "Glyoxal-derived advanced glycation end products (GO-AGEs) with UVB critically induce skin inflammaging: in vitro and in silico approaches," *Sci. Rep.*, vol. 14, no. 1, pp. 1–13, 2024, doi: 10.1038/s41598-024-52037-z.

[37] A. Salminen, K. Kaarniranta, and A. Kauppinen, "Photoaging: UV radiation-induced inflammation and immunosuppression accelerate the aging process in the skin," *Inflamm. Res.*, vol. 71, no. 7–8, pp. 817–831, 2022, doi: 10.1007/s00011-022-01598-8.

[38] M. Modéjar-lópez *et al.*, "Chitosan nanoparticles loaded with garlic essential oil : A new alternative to tebuconazole as seed dressing agent," *Carbohydr. Polym.*, vol. 277, no. 118815, 2022, doi: 10.1016/j.carbpol.2021.118815.

[39] X. Liu, P. Wang, Y. X. Zou, Z. G. Luo, and T. M. Tamer, "Co-encapsulation of Vitamin C and β-Carotene in liposomes: Storage stability, antioxidant activity, and in vitro gastrointestinal digestion," *Food Res. Int.*, vol. 136, no. July, p. 109587, 2020, doi: 10.1016/j.foodres.2020.109587.

[40] C. Tan *et al.*, "Liposomes as delivery systems for carotenoids: Comparative studies of loading ability, storage stability and in vitro release," *Food Funct.*, vol. 5, no. 6, pp. 1232–1240, 2014, doi: 10.1039/c3fo60498e.

[41] S. Golmohammadzadeh, F. Imani, H. Hosseinzadeh, and M. R. Jaafari, "Preparation, characterization and evaluation of sun protective and moisturizing effects of nanoliposomes containing safranal," *Iran. J. Basic Med. Sci.*, vol. 14, no. 6, pp. 521–533, 2011.

[42] Ó. Estupiñán *et al.*, "Mithramycin delivery systems to develop effective therapies in sarcomas," *J. Nanobiotechnology*, vol. 19, no. 1, pp. 1–21, 2021,

doi: 10.1186/s12951-021-01008-x.

[43] P. Preetha, A. Srinivasa Rao, and P. Pushpalatha, “Biphasic Drug Delivery In Controlled Release Formulations – A Review,” *Int. J. Pharm. Technol.*, vol. 6, no. 4, pp. 3046–3060, 2015.

[44] G. Mohammadi *et al.*, “Crocin-loaded nanoliposomes: Preparation, characterization, and evaluation of anti-inflammatory effects in an experimental model of adjuvant-induced arthritis,” *J. Drug Deliv. Sci. Technol.*, vol. 74, no. July, p. 103618, 2022, doi: 10.1016/j.jddst.2022.103618.

[45] J. Vega, J. Bonomi-Barufi, J. L. Gómez-Pinchetti, and F. L. Figueroa, “Cyanobacteria and Red Macroalgae as Potential Sources of Antioxidants and UV Radiation-Absorbing Compounds for Cosmeceutical Applications,” *Mar. Drugs*, vol. 18, no. 12, 2020, doi: 10.3390/MD18120659.

[46] J. Chen, F. Li, Z. Li, D. J. McClements, and H. Xiao, “Encapsulation of carotenoids in emulsion-based delivery systems: Enhancement of β-carotene water-dispersibility and chemical stability,” *Food Hydrocoll.*, vol. 69, pp. 49–55, 2017, doi: 10.1016/j.foodhyd.2017.01.024.

[47] C. Soukoulis and T. Bohn, “A comprehensive overview on the micro- and nano-technological encapsulation advances for enhancing the chemical stability and bioavailability of carotenoids,” *Crit. Rev. Food Sci. Nutr.*, vol. 58, no. 1, pp. 1–36, 2018, doi: 10.1080/10408398.2014.971353.

[48] M. Min, C. Egli, R. A. Bartolome, and R. K. Sivamani, “Ex vivo Evaluation of a Liposome-Mediated Antioxidant Delivery System on Markers of Skin Photoaging and Skin Penetration,” *Clin. Cosmet. Investig. Dermatology* , vol. 17, pp. 1481–1494, 2024, doi: 10.2147/CCID.S461753.

[49] M. Guidoni *et al.*, “Liposomal stem cell extract formulation from Coffea canephora shows outstanding anti-inflammatory activity, increased tissue repair, neocollagenesis and neoangiogenesis,” *Arch. Dermatol. Res.*, vol. 315, no. 3, pp. 491–503, 2023, doi: 10.1007/s00403-022-02388-2.

[50] R. Mokdad, C. Seguin, S. Fournel, B. Frisch, B. Heurtault, and A. Hadjsadok, “Anti-inflammatory effects of free and liposome-encapsulated Algerian thermal waters in RAW 264.7 macrophages,” *Int. J. Pharm.*, vol. 614, no. January, 2022, doi: 10.1016/j.ijpharm.2022.121452.

Declaration of Competing Interest

All persons who meet autorship criterio are listed as authors, and all authors certify that they have participated sufficiently in the work to take public responsibility for the contet, including participation in the concept, desing, analysis, writing, or revisión of the manuscript. Furthermore, each autor certifies that this material or similar material has not been and Will not be submitted to or published in any other publication before its appearance in Colloids and Surfaces B: Biointerfaces

Highlights

- Tomafran extract in liposomes shows antioxidant and anti-inflammatory properties.
- Liposomal Tomafran reduces UVB-induced AGEs and UVA-induced ROS in skin cells.
- Liposomes with Tomafran have stable size, PDI, and zeta potential over 30 days.
- Tomafran liposomes exhibit attractive cosmeceutical properties